

# Incorporation of granite cutting sludge in industrial porcelain tile formulations

P. Torres, H.R. Fernandes, S. Agathopoulos, D.U. Tulyaganov, J.M.F. Ferreira\*

*Department of Ceramics and Glass Engineering, University of Aveiro, CICECO, 3810-193 Aveiro, Portugal*

Received 27 June 2003; received in revised form 21 October 2003; accepted 25 October 2003

## Abstract

Granite wastes in the form of sludge, obtained from granite cutting industry, were incorporated in the batch formulations of porcelain tiles. The maximum possible substitution of sludge for feldspar was investigated. Samples of different formulations, in the form of pellets or extruded bars, were produced at both laboratory and pilot-plant scales and characterized throughout all the stages of the production process. The experimental results and their theoretical interpretation show that suitable incorporation of granite sludge can result in porcelain tiles with superior properties, in terms of water absorption (0.07%) and bending strength (> 50 MPa). Sludge incorporation had negligible effect on density, shrinkage and plasticity during all stages of tile-production process, anticipating no modifications in the industrial production line.

© 2003 Elsevier Ltd. All rights reserved.

**Keywords:** Extrusion; Firing; Sludge; Porcelain; Traditional ceramics; Waste materials

## 1. Introduction

Traditional ceramics, such as bricks, or roof and floor tiles, generally feature high heterogeneity due to the wide range of the composition of natural clays used as raw materials in their fabrication. Thereby, there is a high tolerance for incorporating large amounts of suitable wastes as raw materials.<sup>1–5</sup> This fact attracts further importance since ceramic industry, which is classified as heavy industry, consumes huge amounts of diminishing mineral resources.<sup>6–8</sup> Recycling of wastes has unambiguously beneficial environmental and economical impact,<sup>9–13</sup> while high temperature firing can turn wastes, which contain hazardous components, into inert and safe for the health products.<sup>4,14</sup>

Granite cutting industry produces large amounts of solid wastes worldwide, which are expected to increase owing to the fact that the world production of granite industry has been increasing annually at a rate of 6% in the recent years. The wastes of this industrial activity can reach even 20 or 25 wt.% of the raw granite.<sup>15</sup> Evidently, deposition of huge amounts of granite sludge wastes creates necrotic conditions for flora and fauna

while, after drying, fine particles can be deposited in the lungs of mammals via breath.

Granite sludge is a mixture of debris residue of cut granite rocks with wear remains of cutting steel blades, abrasive metallic shot, and hard materials from the polishing bricks. In the common granite cutting practice, the abrasive metallic shot is dispersed in  $\text{Ca}(\text{OH})_2$  aqueous slurry for cooling. This slurry is continuously pumped and wets all around the granite block slits. Hence, granite sludge contains mainly  $\text{SiO}_2$ ,  $\text{Al}_2\text{O}_3$ ,  $\text{Fe}_2\text{O}_3$  and  $\text{CaO}$ .

In the light of recycling, this work investigates the potential profit of incorporation of granite wastes as raw materials in porcelain-tile industrial formulations, particularly with regards to the following environmental and economical aspects:

- (a). Maximization of the use of granite-sludge waste in porcelain tile production, which would reduce both the environmental impact and the production cost of porcelain tiles.
- (b). Maintenance and if possible improvement of the properties of the produced porcelain tiles. There is still no ISO-standard for the extruded porcelain tiles, which would more interest the present work. Therefore, the produced materials were evaluated in the light of the ISO standard 13006, Group B-I, which is directed to the porcelain tiles made by dry-powder

\* Corresponding author. Tel. +351-234-370242; fax: +351-234-425300.

E-mail address: [jmf@cv.ua.pt](mailto:jmf@cv.ua.pt) (J.M.F. Ferreira).

pressing, whereby water absorption must be less than 0.5% and three point bending strength higher than 35 MPa.<sup>16</sup> Meanwhile, sludge incorporation must not jeopardize materials' properties at the intermediate stages of production process. Otherwise, extended and costly modifications in the industrial production line would be necessary (e.g. size and speed of caring belts, storing and transportation facilities from one unit to another etc.).

In this work, the granite sludge (hereafter denoted as GS) was kindly offered by the industry "Incoveca" (Viseu, Portugal). For comparison purposes, the raw material of commercial porcelain with the trade name Keratec® (K) was used as reference material, made in the porcelain-tile industry "Keratec" (Vagos, Portugal). This industry kindly offered the raw materials and their production line facilities for this work.

The raw materials used in the production of Keratec® porcelain tiles are feldspar (F) and two types of clays, denoted as clay-E (E), which aims to provide plasticity to the green body, and clay-A (A), which provides strength. This work aimed to maximize the replacement of the expensive feldspar with granite sludge. Samples of different compositions in the form of pellets and extruded bars were prepared. The crucial properties were monitored in all the stages of production line until the final product, with respect to the aforementioned aspect (b). The properties of the resulting materials are evaluated in the light of the requirements of the regulations of the ISO-13006 as well as the influence of granite sludge in the mechanism (i.e. phase transformation) of porcelain formation.

During the past few decades, the replacement of feldspar gained increasing acceptance in industry.<sup>17–23</sup> Feldspar is a flux that aims at lowering the vitrification temperature of ceramic bodies during firing and aiding the formation of glassy phase. The composition (in wt.%) of a typical commercial feldspar is ~68% SiO<sub>2</sub>, 19% Al<sub>2</sub>O<sub>3</sub>, 7% Na<sub>2</sub>O, 4% K<sub>2</sub>O, 1% CaO and 0.08% Fe<sub>2</sub>O<sub>3</sub>. Pure potassium feldspar typically contains ≥10% K<sub>2</sub>O.<sup>23,24</sup>

In the literature, there are few reports dealing thoroughly with the involvement of granite sludge wastes in porcelain production. Ferreira et al.<sup>1,11</sup> have shown that the physico-chemical characteristics of granite sludge match well the requirements needed in brick and roof tile formulations. Thus, their incorporation results in negligible changes in the properties of the final products. Menezes et al. have extensively reported the production of bricks and tiles using granite sludge.<sup>5</sup>

## 2. Materials and experimental procedure

The experimental procedure was as follows. The as-received powder of GS was mixed with water in order to

make possible vibratory sieving (90 µm). The sieved mud was dried (110 °C) and then disagglomerated in a hammer-mill. Fourteen different formulations were prepared by mixing of the collected GS powder with the as-received powders of clays A and E and feldspar (F) (Table 1). After this point, commercial powder from Keratec® (K), whose composition is upon trade protection, was also similarly used for comparison purposes. The mixtures were homogenized by addition of water and ultrasonic agitation, dried (110 °C), and disagglomerated by gently grinding in an agate mortar.

Pellets (Ø 20 mm, thickness 2 mm), prepared by cold uniaxial pressing at 47 MPa, were sintered in a laboratory furnace at 1140, 1180, and 1200 °C for 1 h in air (heating-cooling rate 5°/min). Water absorption was measured according to the ISO-standard 10545-3, i.e. weight gain of dried pellets after immersion into boiling water for 2 h, cooling for 3 h and sweeping of their surface with a wet towel.<sup>25</sup> The best formulations were selected according to the following criteria: (a) Water absorption <0.5%, (b) the maximum incorporation of GS, and (c) suitable colour for fabricating commercial porcelain tiles.

Then, the production was upgraded to pilot-plant scale. Batches of ~6 kg of the selected formulations (and Keratec® powder) were mixed with water (~16–19 wt.%) and homogenized using a mixer. The extrusion capability (i.e. plasticity) of the resulting pastes was evaluated with the Pfefferkorn test (i.e. impact effect on a cylinder of the paste with standard dimensions). Extruded cylinders (Ø ~10 mm, length 120 mm) were obtained according to industrial standards (laboratory extruder NR Burton on Trent, Rawdon Ltd., Moira, UK), dried (room temperature-24h, 110 °C-24 h), and fired in the industrial kiln (110 m length, total firing cycle 90 min). The actual sintering temperature in the kiln was that one given by process temperature control

Table 1  
The proportion of the blends for the 14 tested formulations (in wt.%)

Formulation	Clay A	Clay E	Feldspar (F)	Sludge (GS)
1	20	30	0	50% GS
2	25	25	0	
3	20	25	5	
4	15	30	5	
5	50% clay		30	20
6	(20% A + 30% E)		25	25
7			20	30
8			15	35
9			10	40
10			5	45
11	60% clay		20	20
12	(24% A + 36% E)		15	25
13			10	30
14			5	35

rings ( $T_{\text{PTCR}}$ ) (Ferro Electronic Materials B.V, Uden, the Netherlands), whose accuracy (tested in the laboratory furnace with a Pt/Pt–Rh thermocouple) was  $\pm 3^\circ$ . Thus, the apparent sintering temperature in the kiln was fixed at  $T_k = 1210^\circ\text{C}$  but the actual sintering temperature was  $T_{\text{PTCR}} \approx 1185^\circ\text{C}$ .

Several types of characterization tests were conducted during the entire process. The following techniques, together with the aforementioned water absorption and Pfefferkorn tests, were employed. Density of powders and bulk samples was determined by Archimedes' method with water- and Hg-immersion, respectively. Particle size distribution was determined by both conventional sieving and light scattering (Coulter LS 230, UK, Fraunhofer optical model). X-ray diffraction analysis (XRD, Rigaku Geigerflex D/Mac, C Series, Cu  $K_\alpha$  radiation, Japan). X-ray fluorescence analysis (XRF, Model XRF-1700, Shimadzu Corp., Tokyo, Japan). Differential (DTA) and gravimetric (TG) thermal analysis (Labsys Setaram TG-DTA/DSC, France, heating rate  $5^\circ/\text{min}$ , 1 atm flowing  $\text{N}_2$ ). Dilatometer thermal analysis (Bahr Thermo Analyse DIL 801 L, Germany, heating rate  $10^\circ/\text{min}$ ). Scanning electron microscopy (SEM, Hitachi S-4100, 25 kV acceleration voltage, Tokyo, Japan). The presenting results for the three-point bending strength (Shimadzu Autograph AG 25 TA, 0.5 mm/min displacement) are the average of more than 10 tested cylinders. Retraction and weight loss measurements during drying and sintering were also carried out.

In order to shed light to the path of phase transformation during the production processing, quenching experiments were carried out by rapid immersion of pellets, made of the selected formulations and heated at  $5^\circ/\text{min}$  rate and soaked at  $1200^\circ\text{C}$  for 1 h, into cold water. These experiments gave also information for the thermal shock resistance.

### 3. Results

#### 3.1. Raw materials

In order to understand the influence of the incorporation of granite sludge as a raw material for porcelain-tile production, the first stage of this investigation was directed to the complete characterization of all raw materials used in the formulations, A, E, F, and GS, as summarized in Table 2 and Figs. 1–4.

The powders of the raw materials had similar density (clay-A 2.65, clay-E 2.50, feldspar 2.54, and granite sludge  $2.51\text{ g cm}^{-3}$ ). Except A, the size of particles was actually  $< 100\text{ }\mu\text{m}$ , following an almost Gaussian distribution of a single peak, centred between 5 and  $20\text{ }\mu\text{m}$  (Fig. 1).

XRD spectra (Fig. 2) showed well crystallized phases. Quartz ( $\text{SiO}_2$ ), albite (sodium feldspar,  $\text{NaAlSi}_3\text{O}_8$ ),

Table 2

Chemical composition of the raw materials (in wt.%)

Oxide	Clay A	Clay E	Feldspar (F)	Sludge (GS)
$\text{SiO}_2$	64.69	64.87	72.29	71.65
$\text{Al}_2\text{O}_3$	27.91	29.79	16.72	14.25
$\text{Fe}_2\text{O}_3$	2.39	1.75	0.31	2.86
CaO	0.19	0.10	0.71	1.83
MgO	0.58	0.34	0.20	0.86
$\text{Na}_2\text{O}$	0.80	0.65	5.79	3.72
$\text{K}_2\text{O}$	2.43	1.70	3.22	4.43
$\text{TiO}_2$	0.93	0.72	0.02	0.24
MnO	0.01	0.01	0.02	0.03
$\text{P}_2\text{O}_5$	0.07	0.07	0.72	0.13

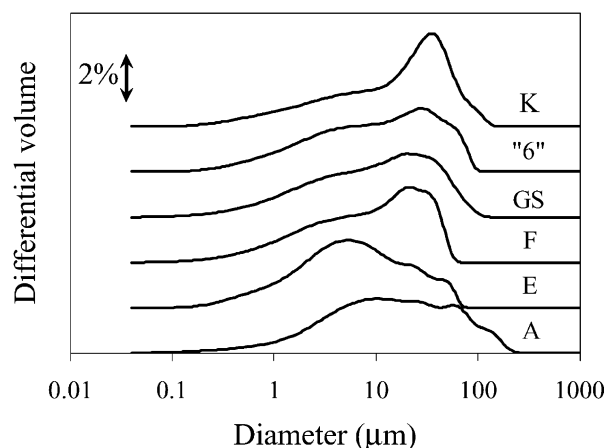


Fig. 1. Particle size distribution of the as-received A, E, F, and the sieved GS powders, together with the powders Keratec<sup>®</sup> (K) and formulation 6 (see Table 1).

illite ( $(\text{K},\text{H}_3\text{O})\text{Al}_2\text{Si}_3\text{AlO}_{10}(\text{OH})_2$ ) and microcline (potassium feldspar,  $\text{KAlSi}_3\text{O}_8$ ) were identified in all powders. Peaks of kaolinite ( $\text{Al}_2\text{Si}_2\text{O}_5(\text{OH})_4$ ) were detected in GS and both clays A and E. Magnetite ( $\text{Fe}^{2+}\text{Fe}_2^{3+}\text{O}_4$ ) was found in GS, while calcite ( $\text{CaCO}_3$ ) in the clays.<sup>26</sup> According to Table 2,  $\text{SiO}_2$  dominates in the sludge (GS), followed by  $\text{Al}_2\text{O}_3$ , while there are high amounts of sodium and potassium oxides, together with calcium and iron oxides too. Evidently, the high CaO-content in GS is mostly due to the  $\text{Ca}(\text{OH})_2$  slurry used to carry the abrasive metallic shot. At this point, it should be noticed that the composition of F matches the composition of pegmatite (i.e. the rock formed by feldspar and quartz),<sup>23</sup> but for simplicity reasons, in this article this component will keep being referred as feldspar (F), since this was the trade name used in industry.

The thermal analyses actually sort out two groups, GS and F, and clay A and E (Fig. 3). The former group showed higher stability over temperature whereas the clays showed a strong endothermic peak and significant weight loss at  $530\text{--}550^\circ\text{C}$ . In the case of clays, careful observation might suggest two more weak exothermic

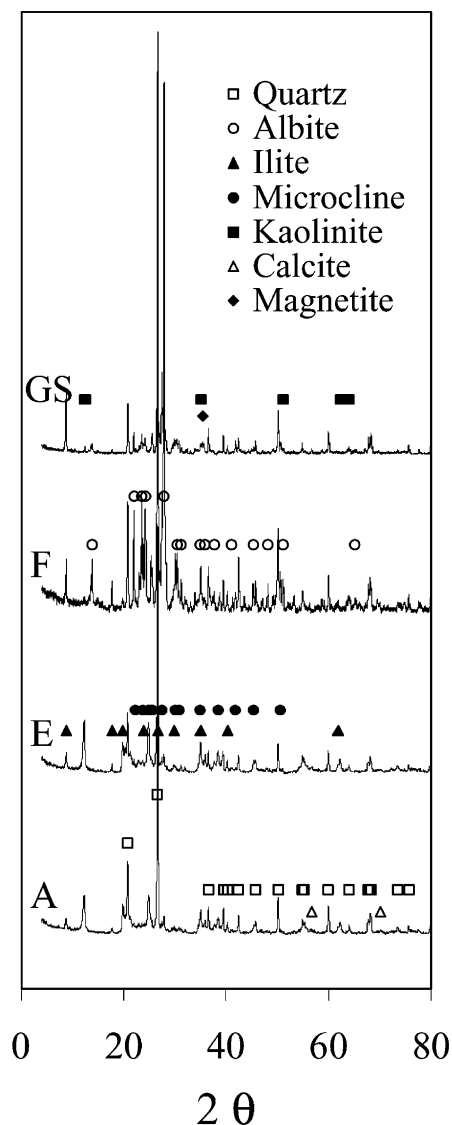


Fig. 2. XRD spectra of the A, E, F, and GS (the position of the peaks of the phases are also marked<sup>26</sup>).

peaks, at 950–980 °C and 1120–1150 °C (for clay A). For the GS, a weak endothermic peak might be suggested at 570–580 °C, probably due to the transformation of  $\alpha$ - to  $\beta$ -quartz.<sup>27</sup> The clays also underwent a slight weight loss at ~600–700 °C.

The same grouping (i.e. GS–F and A–E) seemingly reflects the water absorption capability of pellets sintered between 1140 and 1200 °C for 1 h, where the clays absorb 5–10 times more water than F or GS (Fig. 4).

### 3.2. Selection

Fig. 5 depicts the water absorption of pellets made of the formulations listed in Table 1, together with the reference composition of Keratec® (K) sintered at 1140, 1180, and 1200 °C for 1 h. Evidently, water absorption decreases up to 1180 °C due to densification process,

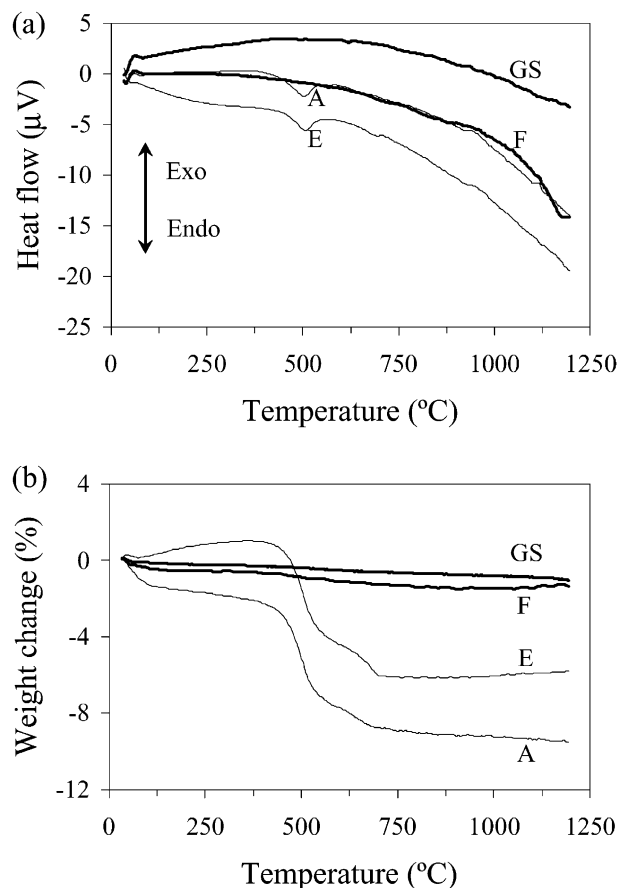


Fig. 3. Thermal analysis, (a) DTA, (b) TG, for the A, E, F, and GS.

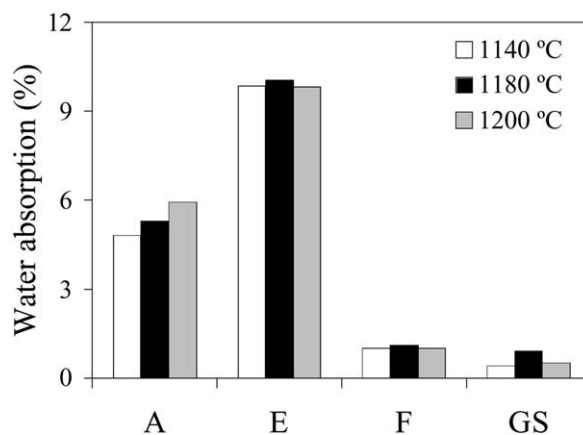


Fig. 4. Water absorption for pellets made of the A, E, F, and GS, sintered at different temperatures for 1 h.

and then increases again likely due to an over-firing effect. In general, all samples satisfied the three selection criteria mentioned in the “materials and experimental procedure” section, especially those sintered at higher temperatures. Therefore, a fourth selection criterion was introduced, basing on the lower water absorption level achieved at the lowest sintering temperature. Accordingly (Fig. 5), the selected formulations were those with the numbers 3, 5, 6, 7, 8 and 9 (Table 1).

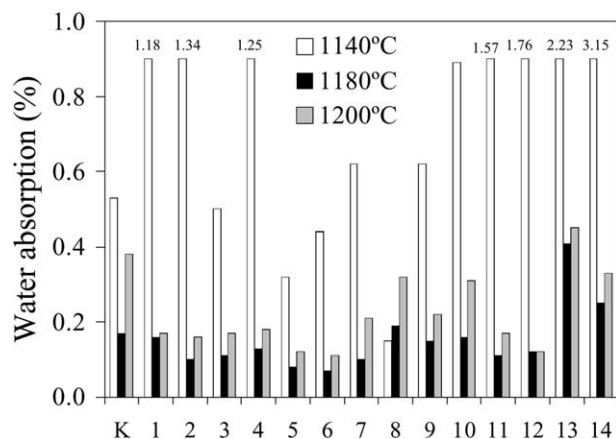


Fig. 5. Water absorption of the pellets with the formulations listed in Table 1 and Keratec® (K), fired at different temperatures for 1 h.

### 3.3. Extruded bars

The particle size distribution curves of the blends made of the selected formulations resemble those of the raw materials (Fig. 1, all the selected formulations showed similar distribution to that of formulation 6). In accordance to the plasticity (Pfefferkorn) tests (Fig. 6), extruded cylinders were perfectly obtained from the moistened pastes, whose water content is shown in Table 3.

It should be noticed that muscovite ((K,Na)(Al,Mg,Fe)<sub>2</sub>(Si<sub>3.1</sub>Al<sub>0.9</sub>)O<sub>10</sub>(OH)<sub>2</sub>)<sup>26</sup> was identified in the green extruded cylinders (including Keratec®) (Fig. 7), though it was not identified in the raw materials (Fig. 2). Therefore, it is suggested that the powders of the raw materials (mostly the clays) contained randomly orientated muscovite but the extrusion aligned the muscovite layers along the extrusion direction, intensifying mainly the peak at 8.9°, which according to the JCPDS card 07-0042 is assigned to the plane 003. The X-ray diffraction of the planes corresponding to the 006, 101 or 100, 112, 115, and 1111 planes might be also suggested

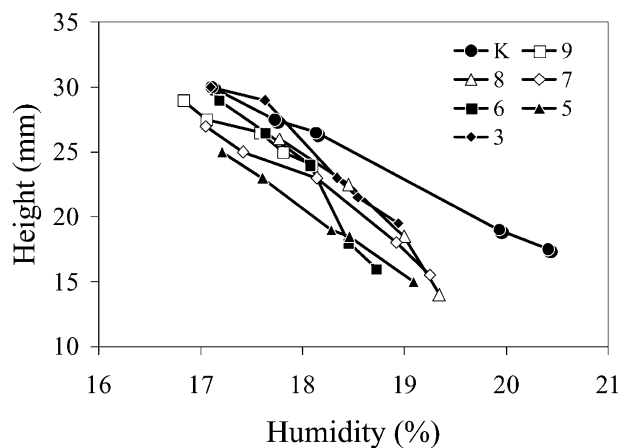


Fig. 6. Plasticity curves for the six selected formulations and Keratec® (K) (Pfefferkorn test).

(Fig. 7), while the second principal peak of muscovite (26.7°) is hardly distinguished from the principal peak of quartz (26.6°). In layer structured materials, the alignment of crystallites has been reported in tape casting or extrusion.<sup>28</sup>

The extruded cylinders perfectly survived drying and firing. Table 3 summarizes the values of the properties of the extruded cylinders and particularly the retraction and weight loss during drying and sintering, the bending strength and the density of both green and fired bodies and the water absorption of the sintered ceramics. Evidently, the investigated formulations had superior properties mainly with regards to water absorption as well as bending strength. On the other hand, except formulation 3, sludge incorporation had negligible effect on the other properties with respect to the commercial porcelain (K). It should be also underlined that there was an effort for approaching the optimum sintering temperature (i.e. 1180 °C, which showed the lowest water absorption values, Fig. 5) also in the industrial kiln. Therefore, since it was not advisable to change for long the industrial sintering schedule for merely an experimental testing, the best approach of this temperature was  $T_{\text{PTCR}} \approx 1185$  °C.

Fig. 7 reveals the phase transformation taken place during firing and cooling for the formulations 6 and K, (all the other tested formulations showed similar XRD spectra to that of formulation 6).<sup>26</sup> In general, firing resulted in the formation of mullite and glassy phase, with some non-dissolved quartz still remaining in the sintered bodies. Traces of un-reacted albite were scarcely identified (not shown here). The XRD patterns of the quenched samples (not shown here) revealed an intermediate regime (i.e. increasing glassy phase and presence of traces of the crystalline phases of the green body together with mullite), evidencing that the final crystalline structure is established after the slow cooling.

Fig. 8 plots the results of the thermal analyses for the formulation 3 and K. In a qualitative basis, all the selected formulations showed similar behaviour but the clay-richer formulations underwent more intensive weight loss (not shown here). The important temperatures in both DTA and TG curves coincide with the temperatures mentioned in the presentation of Fig. 3. In general, the investigated formulations (Fig. 8) resemble rather the behaviour of the clays than the GS and the F (Fig. 3). The dilatometry curves of the green samples (not shown here) appear practically superimposed, showing a small expansion up to ~1000 °C where they start to shrink, following not exactly the same but similar paths afterwards.

Fig. 9 shows characteristic microstructures of fired bars observed at the fracture surface after three point bending tests. All of them look very similar, exhibiting good homogeneity when observed at low magnification,



Table 3

Values (and standard deviation) of properties of the selected formulations in comparison with the commercial Keratec® (K) (for samples' identification see Table 1)

Property	Formulation						
	3	5	6	7	8	9	K
<b>Green bodies</b>							
Water content (wt.%)	18.80	17.50	18.88	16.79	16.90	16.82	16.91
Retraction during drying (%)	5.04±0.23	3.88±0.14	5.34±0.25	3.56±0.21	3.87±0.16	2.92±0.14	3.20±0.12
Three-point bending strength (MPa)	3.22±0.18	3.53±0.27	3.43±0.15	2.75±0.16	3.26±0.16	3.28±0.23	3.64±0.08
Density (gcm <sup>-3</sup> )	1.79±0.06	1.81±0.01	1.77±0.01	1.80±0.01	1.83±0.01	1.82±0.01	1.85±0.01
<b>Samples fired in the industrial kiln (<math>T_k = 1210^\circ\text{C}</math>, <math>T_{\text{PTCR}} \approx 1185^\circ\text{C}</math>, 90 min)</b>							
Water absorption (%)	0.08±0.01	0.26±0.01	0.07±0.01	0.13±0.01	0.21±0.08	0.27±0.01	1.31±0.10
Retraction during sintering (%)	7.13±0.14	5.56±0.12	6.45±0.20	5.96±0.11	6.57±0.15	6.78±0.16	6.26±0.22
Weight loss during sintering (%)	4.64±0.03	5.30±0.03	5.36±0.05	5.40±0.04	4.76±0.03	4.62±0.03	5.14±0.06
Three-point bending strength (MPa)	58.26±2.85	60.02±1.92	54.79±2.60	59.21±2.41	60.26±3.29	59.79±2.54	47.84±3.05
Density (gcm <sup>-3</sup> )	2.26±0.01	2.22±0.01	2.20±0.01	2.23±0.01	2.25±0.02	2.27±0.01	2.27±0.01

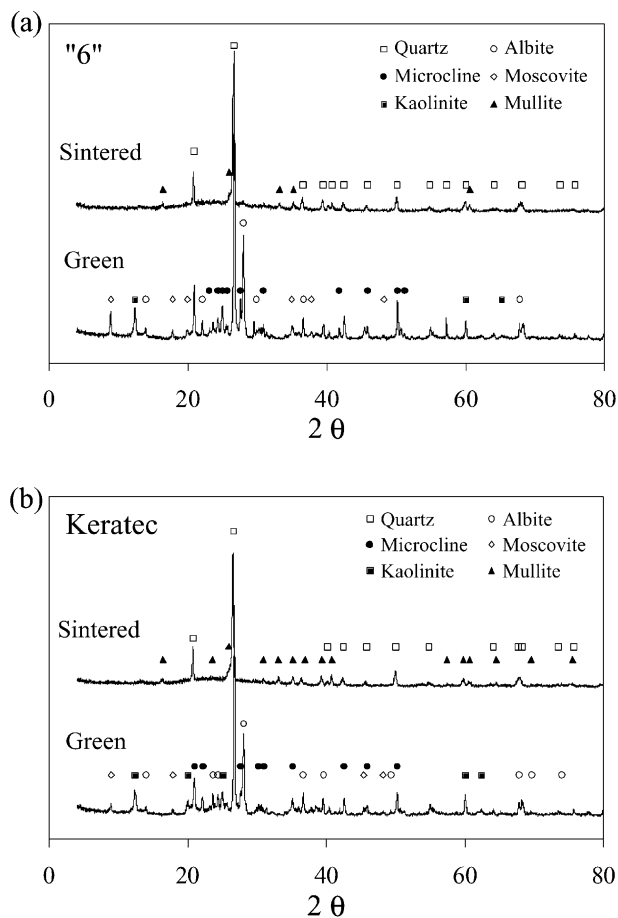


Fig. 7. Crystalline structure (XRD<sup>26</sup>) of dry green body and sintered samples of the formulation 6 and Keratec® (K). All the selected formulations showed very similar patterns.

while, at higher magnification (insets), there were observed spherical pores, typically formed in the glassy phase. These porous microstructures probably reflect a somewhat over-firing effect, which might cause increasing water absorption (Fig. 5).

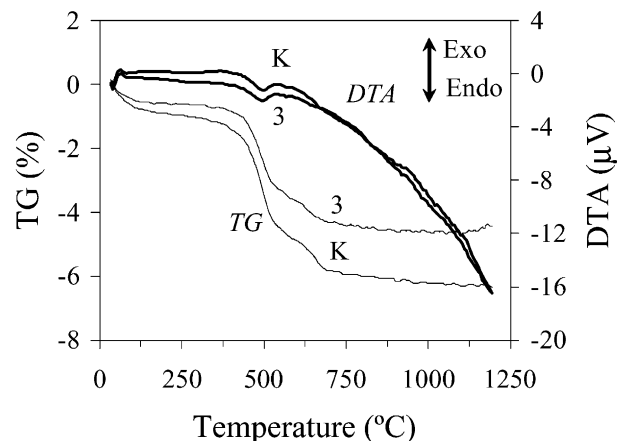


Fig. 8. Thermal analyses (DTA and TG) of the formulation 3 and Keratec® (K). Qualitatively, all the selected formulations showed similar curves, but the clay-richer formulations underwent more intensive weight loss (not shown here).

Finally, it is worthy noting that all the selected formulations showed remarkable thermal shock resistance since they survived quenching and not even a single crack was observed at the surface of the quenched pellets.

#### 4. Discussion

This work is actually directed to the field of designing new ceramic compositions, which can meet certain requirements. Among the wide family of commercial and traditional ceramics, porcelain tiles must satisfy the highest and most strict quality standards, which apparently depend on the high quality of the raw materials and the optimization of the processing parameters. This is however a difficult task due to the use of natural raw materials. Granite is a magmatic and one of the most abundant natural rocks and approximately contains 66 wt.% quartz, (which exposes its acidic behaviour), 26%

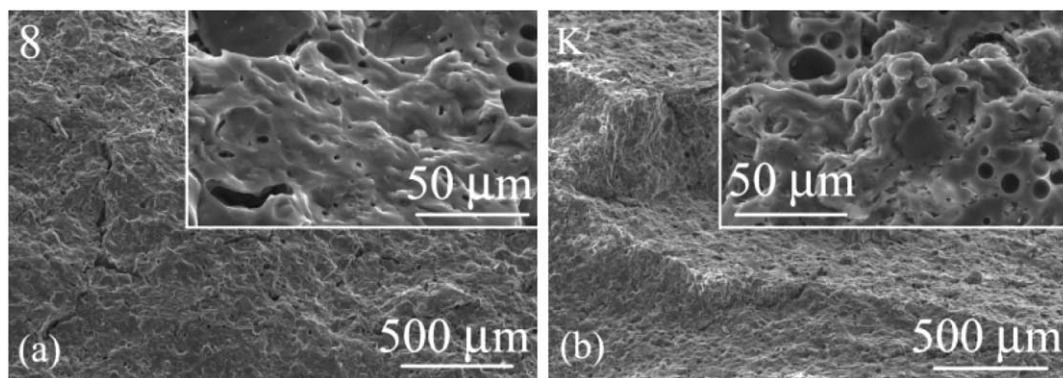


Fig. 9. Characteristic SEM microstructures of extruded cylinders of (a) the formulation 8 and (b) Keratec® (K), observed at the fracture surfaces after three point bending test at low and high magnification (insets). All the selected formulations showed similar microstructures.

feldspar, and 8% mica, together with smaller amounts of clay- and iron-containing minerals. In this particular work, the characteristics of the incorporated granite wastes likely depend on the specific source. For example, the iron content in granite sludge can increase due to residues of cutting steel blades and abrasive metallic shot. Moreover, CaO content may be easily changed if sludge from granite is mixed in any proportion with sludge from marble rocks.

Apparently, each one of the four raw materials mixed in the tested batches (Table 1) contains different amount of fluxes and thus it has a particular contribution to the sintering process. Hence, the optimization of tile formulation should take into account both the chemical composition and the crystalline structure of the raw materials. The proportion of the raw materials in the batch is another important factor. This is clear because of the following fact. This work aimed to maximize the substitution of sludge for the expensive feldspar. However, the best results were achieved when both feldspar and sludge were present, whereas absolute substitution (samples 1 and 2 of Table 1) resulted in materials with poorer properties (Fig. 5).

In order to find a relationship between the composition and the sintering ability of the tested batches, Table 4 presents the composition (in mol%) of the main ( $K_2O$ ,  $Na_2O$ ) and the auxiliary fluxes ( $CaO$ ,  $MgO$ ,  $Fe_2O_3$ ) in F and GS. The total molar fraction for  $K_2O$ ,  $Na_2O$ ,  $CaO$ , and  $MgO$  fluxes is 9.57% for the F and 10.62% for the GS, while GS is also richer than F in another auxiliary flux, i.e.  $Fe_2O_3$  (probably derived from the wearing of metallic cutting steel blades and abrasive metallic shot). Hence, substitution of GS for

F can improve the sintering behaviour because the higher content of fluxes evidently decreases the viscosity of the glassy phase and accelerates the sintering process of ceramic body.<sup>29</sup> On the other hand, the DTA curve of F seemingly ends with a plateau at  $\sim 1150^\circ C$  probably assigned to the melting of feldspar (Fig. 3a). Thus, feldspar melting should precede the melting of granite sludge. Hence, the optimization of the composition requires the presence of both the sludge and the feldspar.

In a qualitative basis, the results of the thermal analyses and the XRDs showed that the commercial Keratec® paste, the clays A and E, and the six selected formulations behave in the same manner (Figs. 3, 7 and 8). Therefore, the firing process should comprise the following stages. Since the clays are constituted of very fine plates with lateral dimensions of 0.1–3  $\mu m$  and thickness 0.5–2  $\mu m$ ,<sup>22,23,30</sup> the water adsorbed at the high specific surface area clay particles is eliminated until 200  $^\circ C$ . Oxidation of organic components takes place until 700  $^\circ C$ , depending on their chemical nature. At 573  $^\circ C$ , quartz is transformed to its high temperature  $\beta$  form. Between  $\sim 450$  and  $\sim 600^\circ C$ , kaolinite loses the chemical bonded water and turns into metakaolinite. The slight weight loss at  $\sim 600$ –700  $^\circ C$  might be ascribed to illite and muscovite minerals.<sup>27</sup> At  $\sim 950^\circ C$ , the lattice is totally collapsed, silica is eliminated and spinel is formed (i.e.  $2(Al_2O_3 \cdot 2SiO_2) \rightarrow 2Al_2O_3 \cdot 3SiO_2 + SiO_2$ ). Spinel is transformed to mullite at  $\sim 1150^\circ C$  (i.e.  $3(2Al_2O_3 \cdot 3SiO_2) \rightarrow 2(3Al_2O_3 \cdot 2SiO_2) + 5SiO_2$ ). It has been reported, however, that the formation of spinel depends on the presence of other admixtures.<sup>23,29</sup>

Theoretically, liquid phase should form at the eutectic temperature of potassium feldspar ( $KAlSi_3O_8$ ) and quartz (985  $^\circ C$ ).<sup>23,29</sup> Amorphous silica, formed during the thermal decomposition of kaolinite, reacts with potassium feldspar. At high temperatures, quartz is dissolved in the liquid phase. In this work, there was no addition of quartz in the batches during the process but quartz was intrinsically incorporated in the clays, the granite sludge, and the feldspar (Fig. 2). For pure

Table 4

Content of fluxes in the feldspar (F) and the granite sludge (GS) (in mol%)

Material	CaO	MgO	Na <sub>2</sub> O	K <sub>2</sub> O	Fe <sub>2</sub> O <sub>3</sub>
F	0.84	0.33	6.15	2.25	0.13
GS	2.15	1.41	3.96	3.10	1.18

potassium feldspar, complete melting should take place at its melting temperature  $\sim 1150^\circ\text{C}$ . It is also mentioned that the eutectic point of sodium feldspar and silica is  $\sim 1062^\circ\text{C}$ , while the melting point of pure albite is  $\sim 1118^\circ\text{C}$ .<sup>27</sup>

As far as the fabrication and commercialization of porcelain tiles are concerned with the incorporation of granite sludge, this work has shown that optimal proportion of the raw materials in the batch and firing at  $\sim 1180^\circ\text{C}$  potentially result in superior porcelain tiles. In particular, the powder of granite sludge featured a symmetrical and wide particle size distribution (between 1 and  $100\ \mu\text{m}$ , Fig. 1), which facilitates high compaction of the final product while mixing in suitable proportions with the other raw materials.<sup>31</sup> The incorporation of the sludge had negligible effect in density, shrinkage and plasticity of materials during all stages of production process. Therefore, expensive modifications in the industrial production line are omitted. On the other hand, the presence of granite sludge considerably lowered the water absorption ( $< 0.25\%$ ) and firmly increased of mechanical strength ( $> 55\ \text{MPa}$ ), comparing to the commercial porcelain (Table 3).

These values make further sense if compared with the earlier work reported by Menezes et al.<sup>5</sup> In that work, the incorporation of granite sludge resulted in bricks and tiles with relatively high water absorption values and poorer flexural strength than the produced porcelains in this work (i.e. 8–17% and 8–23 MPa upon firing at  $1150^\circ\text{C}$ ; 2–8% and 19–36 MPa upon firing at  $1175^\circ\text{C}$ ; 0.4–3.0% and 24–36 MPa upon firing at  $1200^\circ\text{C}$ ). The superior behaviour of the investigated formulations is also evidence by the small differences in water absorption shown for several selected formulations sintered between 1140 and  $1200^\circ\text{C}$  (Fig. 5). In ceramic industry for tile production, this is very important because the crucial goal is the secure broadening of sintering range, with regard to the maintenance of the quality of the product.

At this point it must be underlined that Keratec® commercial porcelains exhibit water absorption definitely lower than 0.5% because they obviously satisfy the ISO regulations. The higher amount of water absorption measured in this work with the K samples is due to the different experimental procedure (i.e. mixing, drying and sintering conditions), comparing to the strict industrial fabrication. The experimental conditions followed in this work purposefully increased the gap between the properties of the tested formulations and the commercial one and thus facilitated their comparison.

The construction sector is the best target market (i.e. bricks, wall and floor tiles) for absorbing and consuming products made of recycling solid wastes which are produced at enormous amount, such as granite or other cutting rock wastes.<sup>1,5</sup> In the particular case of granite, beyond reducing the harmful environmental impact of

deposition of wastes and lowering the production cost of porcelain, it is worthy noting that granite sludge contains no hazardous chemicals but true natural materials, anticipating, therefore, safe for the health an environmentally friendly recycling products.

## 5. Conclusions

- (a). The incorporation of granite sludge wastes in porcelain tile production anticipates safe for the health an environmentally friendly recycling products.
- (b.) Provided that there is optimal proportion of the raw materials in the batch and firing temperature is  $\sim 1180^\circ\text{C}$ , the resulting extruded porcelain items satisfy the closest ISO standard (13006, Group B-I), and can exhibit superior properties comparing to the commercial porcelains, with regards to water absorption, flexural strength, and widening of sintering range.
- (c). The incorporation of granite sludge has negligible effect on the other properties during the entire process, anticipating no costly modifications in the industrial production line.

## Acknowledgements

The financial support of the Project PRAI-Centro, “Caracterização e reciclagem de lamas derivadas do corte de rochas naturais e ornamentais”, Programa Regional de Acções Inovadoras do Centro de Portugal is acknowledged. S.A. acknowledges the financial support of the Portuguese Foundation of Science and Technology under the PRAXIS-XXI grant SFRH/BPD/1619/2000 and D.T. CICECO for the post-doctoral grant.

## References

1. Ferreira, J. M. F., Torres, P. M. C., Silva, M. S. and Labrincha, J. A., Recycling of granite sludges in brick-type and floor tile-type ceramic formulations. *Euroceram News*, 2003, **14**, 1–5 [http://www.euroceram.org/en/news/news\\_14\\_1.cfm](http://www.euroceram.org/en/news/news_14_1.cfm).
2. Ribeiro, M. J., Ferreira, J. M. F. and Labrincha, J. A., Incorporation of clay-based ceramic formulations containing different solid wastes. *Euroceram News*, 2003, **14**, 1–4 [http://www.euroceram.org/en/news/news\\_14\\_2.cfm](http://www.euroceram.org/en/news/news_14_2.cfm).
3. Knirsch, M., Penschke, A., Krebs, S., Ruß, W., Mörtel, H., Mayer, W. A. and Mayer-Pittroff, R., Application of brewery wastes in the production of bricks. *Tile & Brick Int.*, 1998, **14**, 93–101.
4. Ferreira, J. M. F., Alves, H. M. and Mendonça, A. M., Inertization of galvanic sludges by its incorporation in ceramic products. *Boletín de la Sociedad Española de Cerámica y Vidrio*, 1999, **38**, 127–131.
5. Menezes, R. R., Ferreira, H. S., Neves, G. A. and Ferreira, H. C.,



- The use of granite wastes as ceramic raw materials. *Cerâmica*, 2002, **48**, 92–101 (in Portuguese).
6. Martins, O. R., Grandes linhas do comportamento mundial da indústria e do comércio das rochas ornamentais em 1996. *Boletim de Minas*, 1998, **35**, 123–149 (in Portuguese).
  7. Vieira, T. and Sobreiro, M. J., Rochas ornamentais e industriais Portuguesas. (elementos estatísticos de 1997). *Boletim de Minas*, 1999, **36**, 375–390 (in Portuguese).
  8. Moura, A. C., A pedra natural ornamental em Portugal—nota breve. *Boletim de Minas*, 2001, **38**, 161–177 (in Portuguese).
  9. Boccacini, A. R., Schawohl, J., Kern, H., Schunck, B., Rincon, J. M. and Romero, M., Sintered glass ceramics from municipal incinerator fly ash. *Glass Technol.*, 2000, **41**, 99–105.
  10. Gorokhovskiy, A., Gorokhovskiy, V. and Mescheryakov, D., Glass-ceramic materials based on complex utilization of industrial wastes: structural features. *Glass Sci. Technol.*, 2000, **73**, 374–377.
  11. Ferreira, J. M. F., Torres, P. M. C., Silva, M. S. and Labrincha J. A., Recycling of sludges generated from natural stones cutting processes in ceramic formulations. In *Proceedings of the Recycling and Waste Treatment in Mineral and Metal Processing: Technical and Economic Aspects*, ed. B. Björkman, C. Samuelsson, and J.O. Wikström. Luleå University of Technology, Luleå-Sweden, 2002, pp. 389–396.
  12. Ferreira, J. M. F., Guedes, P. J. S. and Faim, P. F., Recycling of industrial residues: the best strategy for waste management. *Al-Azhar Bulletin of Science*, 2003, **March**, 293–305.
  13. Ferreira, J. M. F. and Olhero, S. M., Al-rich sludge treatments towards recycling. *J. Eur. Ceram. Soc.*, 2002, **22**, 2243–2249.
  14. Ferreira, J. M. F., Olhero, S., Lemos, A. and Xavier V., Suitability of the ceramic matrixes for recycling industrial inorganic wastes. In *Proceedings of the Recycling and Waste Treatment in Mineral and Metal Processing: Technical and Economic Aspects*, ed. B. Björkman, C. Samuelsson and J.O. Wikström. Luleå University of Technology, Luleå-Sweden, 2002, pp. 369–375.
  15. Fernandes, H. R., Torres, P., Agathopoulos, S., Tulyaganov, D. and Ferreira, J. M. F., Utilization of solid wastes from granite cutting processing in porcelain industry. *Al-Azhar Bulletin of Science*, 2003, **March**, 33–43.
  16. Ceramic Tiles—Definition, classification, characteristics and marking. International Organization for Standardization, ISO 13006, 1998.
  17. Sanchez, E., Garcia, J., Sanz, V. and Ochandio, E., Raw material selection criteria for the production of floor and wall tiles. *Tile & Brick*, 1990, **6**, 15–21.
  18. Sandoval, F. and Ibañez, A., Fast firing wollastonite-based wall tile bodies. *Am. Ceram. Soc. Bull.*, 1999, **78**, 72–75.
  19. Taspinar, B. and Ay, N., Use of perlite in wall tile production. *Am. Ceram. Soc. Bull.*, 1999, **78**, 86–87.
  20. Rokhvargher, A. E. and Khizh, A. B., Conveyer technology for tile and other thin-walled ceramics. *Am. Ceram. Soc. Bull.*, 1998, **77**, 59–75.
  21. Bozadgiev, L., Porcelain on bulgarite basis. *Interceram*, 2000, **49**, 8–10.
  22. Ryan, W., *Properties of Ceramic Raw Materials*, 2nd ed. Pergamon press, New York, 1978.
  23. Avgustinik, A. I., *Ceramics*, 2nd ed. Stroiizdat, Leningrad, Russia, 1975 (in Russian).
  24. Annual Minerals Review, *Am. Ceram. Bull.*, 1999, **78**, 131.
  25. Ceramic Tiles—Part 3. International Organization for Standardization, ISO 10545-3, 1995.
  26. JCPDS cards: quartz: 46-1045; microcline: 19-0932; albite: 09-0466; ilite: 26-0911; kaolinite: 29-1488; calcite: 05-0586; magnetite: 19-0629; mullite: 15-0776; muscovite: 07-0042.
  27. Jouenne, C. A., *Traité de Céramiques et Matériaux Minéraux*. Editions Septima, Paris, 1975.
  28. Grim, R. E., *Applied Clay Mineralogy*. McGraw-Hill, New York, 1962.
  29. Budnikov, P. P., *The Technology of Ceramics and Refractories*. MIT press, Cambridge, Mass, 1972.
  30. Carty, W. M., The colloidal nature of kaolinite. *Am. Ceram. Soc. Bull.*, 1999, **78**, 72–79.
  31. Ortega, F. S., Pileggi, R. G., Sepulveda, P. and Pandolfelli, V. C., Optimizing particle packing in powder consolidation. *J. Am. Ceram. Soc.*, 1999, **78**, 106–111.